Eur Arch Otorhinolaryngol (2016) 273:3759–3764
DOI 10.1007/s00405-016-4064-8

RHINOLOGY

A study of the anterior ethmoidal artery and a new classification of the ethmoid roof (Yenigun classification)

Alper Yenigun[1] · Seda Sezen Goktas[1] · Remzi Dogan[1] · Sabri Baki Eren[1] · Orhan Ozturan[1]

Received: 2 February 2016 / Accepted: 19 April 2016 / Published online: 26 April 2016

Abstract Aims of this study are to analyze the association of the anterior ethmoidal artery's (AEA) visualization with variations in its adjacent structures in coronal, axial, and sagittal CT images, to assess its relation with the ethmoid roof, and, based on this relation, to introduce a new classification for the ethmoid roof. A retrospective, cross-sectional study was performed in a tertiary referral center. In this retrospective, cross-sectional study, the coronal, axial, and sagittal CTs of 184 patients have been surveyed and the AEA canal, the ethmoid roof, and their relations with surrounding structures have been assessed. The Keros classification used to measure the depth of the lateral lamella of the cribriform plate (LLCP) in the ethmoid roof has been modified to include anterior–posterior length of the LLCP. It was shown that the visualization of the AEA canal increases in a statistically significant manner with an increase in the superior–inferior depth and the anterior–posterior length of the LLCP bilaterally. In the presence of supraorbital pneumatization, AEA visualization was shown to increase bilaterally significantly. This study demonstrated a positive correlation between the AEA canal, the LLCP superior–inferior depth, and the anterior–posterior length. It was shown that with the increased depth and length of the LLCP and in the presence of supraorbital pneumatization, the visualization of the artery and hence the injury risks are increased. The LLCP anterior–posterior length is as clinically relevant as is its depth, and a radiologic classification has been defined according to the anterior–posterior length of the LLCP.

Keywords Anterior ethmoidal artery · Computed tomography · Keros classification · Ethmoid roof

Abbreviations

AEA	Arteria ethmoidalis anterior
CSF	Cerebrospinal fluid
CT	Computed tomography
DSA	Digital subtraction angiography
ESS	Endoscopic sinus surgery
LLCP	Lateral lamella of the cribriform plate
SOP	Supraorbital pneumatization

Introduction

Endoscopic sinus surgery (ESS) is a recognized approach to sinonasal pathologies. During surgery, given the proximity between the sinuses and the eyes and brain, close attention needs to be paid to sinonasal anatomy and its variations [1]. While ESS is undertaken commonly, there are two groups of minor and major complications. Minor complications, such as bleeding, infection, incrustation, synechiae, and recurrence are seen in 1.1–20.8 % of cases, while major complications, including cerebrospinal fluid leak, ocular and orbital injury, or intracranial trauma are observed in 0–1.5 % of cases [2].

The roof of the ethmoidal labyrinth is formed by the fovea ethmoidalis, a segment of the frontal bone separating the ethmoid cells from the anterior cranial fossa. Where the fovea ethmoidalis inserts at the skull base, the lateral

✉ Alper Yenigun
alperyenigun@gmail.com

[1] Department of Otorhinolaryngology, Faculty of Medicine, Bezmialem Vakif University, Adnan Menderes Bulvarı Vatan Caddesi, 34093 Fatih, Istanbul, Turkey

lamella of the cribriform plate (LLCP), the thinnest bone of the skull base was found [3]. This is the region most likely to be injured during surgery [1]. In 1962, Keros characterized three categories of cribriform plate according to its depth and position relative to the ethmoid roof [4].

The anterior ethmoidal artery (AEA), a branch of the ophthalmic artery, arises from the internal carotid artery. The AEA runs along the so-called anterior ethmoidal sulcus in the lateral lamella, the narrowest section of the anterior skull base, and reaches the olfactory fossa [5]. At this point, the bone is extremely thin and the AEA's position relative to the ethmoid roof shows variability; hence, the injury risk in ESS is elevated [6, 7]. Computed tomography has been described as the best method for the visualization of the paranasal sinuses and related structures [8].

The aim of this study was to investigate the relation between AEA visualization and variations of the skull base, assess the relation with the ethmoidal roof, and develop a new classification scheme for the skull base on the basis of this relation considering antero-posterior length of LLCP.

Methods

This is a retrospective study, approved by the local Clinical Research Ethics Committee, evaluating axial paranasal sinus CT (Philips Brilliance 64-slice CT scanner, Philips Medical Imaging, The Netherlands) images, taken in 2 mm sections. The axial CT scans were performed on patients positioned supinely; the patients' head position was adjusted in such a way that the hard palate was parallel to the floor, while the sagittal plane was perpendicular to the floor. All CT images had been ordered for sinonasal, otologic or maxillofacial inquiries between January 2014 and January 2015. Patients with nasal polyposis or sinus anomalies and those who had undergone previous sinus surgery were excluded from the study.

In 184 patients, according to CT findings AEA visualization was assessed in relation to the superior–inferior depth of the cribriform plate (Keros classification), the anterior–posterior length of the cribriform plate, supraorbital pneumatization, pneumatization of the crista galli, agger nasi, concha bullosa, and septum deviation.

In assessing the AEA visualization, on the paranasal CTs we followed the AEA canal, tracking the bilateral medial notch and the ethmoid sulcus in the cribriform plate.

To assess the superior–inferior depth of the cribriform plate, we used the Keros classification (type 1: 0–3 mm, type 2: 4–7 mm, type 3: 8–16 mm) in the coronal section [4].

To adapt Keros' classification made in the coronal section to the anterior–posterior length in the axial section, we defined a "Yenigun classification". This classification measures the expected level of the artery by trying to trace the ethmoid sulcus in the axial section, either from the level of the artery seen between the orbita and skull base or, in case the artery has not been selected entirely, from the orbital notch medially and from the cribriform plate laterally. For this measurement, the endpoint of the crista galli has been accepted as posterior boundary. In our measurements, the length of the cribriform plate ranged between a minimum of 6 mm and a maximum of 20 mm; we classified the anterior–posterior length of the cribriform plate into type 1: 6–10 mm (Fig. 1a), type 2: 11–15 mm (Fig. 1b), and type 3: 16–20 mm (Fig. 1c).

The data were evaluated statistically by Chi square test. Differences at the level of $p < 0.05$ were accepted to be statistically significant.

Results

Of the 184 patients (368 sides) assessed through CT of the paranasal sinus taken in axial, coronal, and sagittal plane, 116 (63 %) were male and 68 (37 %) female. The ages of the cases ranged between 13 and 76 years, the average being 35.31 ± 13.79 years.

Evaluating the distribution of AEA visualization on the 184 patients' CTs, the images showed a visible course of the AEA inside the ethmoid sinus in 53.2 % (right: 53.8 %, left: 52.7 %) of cases, while in 46.7 % (right: 46.2 %, left: 47.3 %), the AEA was directly penetrating the skull base.

Table 1 shows the relationship between the course of the AEA being visible inside the ethmoid sinus as seen on the CTs and the type according to the Keros classification. What is striking in Table 1 is that with increasing depth of the cribriform plate according to the Keros classification, the AEA visualization also increases. As the depth of the cribriform plate according Keros classification decreases, the probability for AEA directly to penetrate the skull base rises steeply. This correlation has been found statistically significant (right: $p = 0.00$; left: $p = 0.00$) (Tables 1, 2).

In the CT distribution, in the 184 patients the types of anterior–posterior length of the cribriform plate (Yenigun classification) were observed to be 41.8 % (right: 42.5 %, left: 41.1 %) for type 1, 53.3 % (right: 52.0 %, left: 54.6 %) for type 2, and 4.9 % (right: 5.1 %, left: 4.7 %) for type 3. Table 1 shows the relationship between the visible course of the AEA inside the ethmoid sinus as seen on the CTs and the type according to the Yenigun classification. What is striking in Table 1 is that with increasing length of the cribriform plate according to the Yenigun classification, the AEA visualization also increases. As the length of the cribriform plate according to the Yenigun classification decreases, the probability for AEA directly to penetrate the

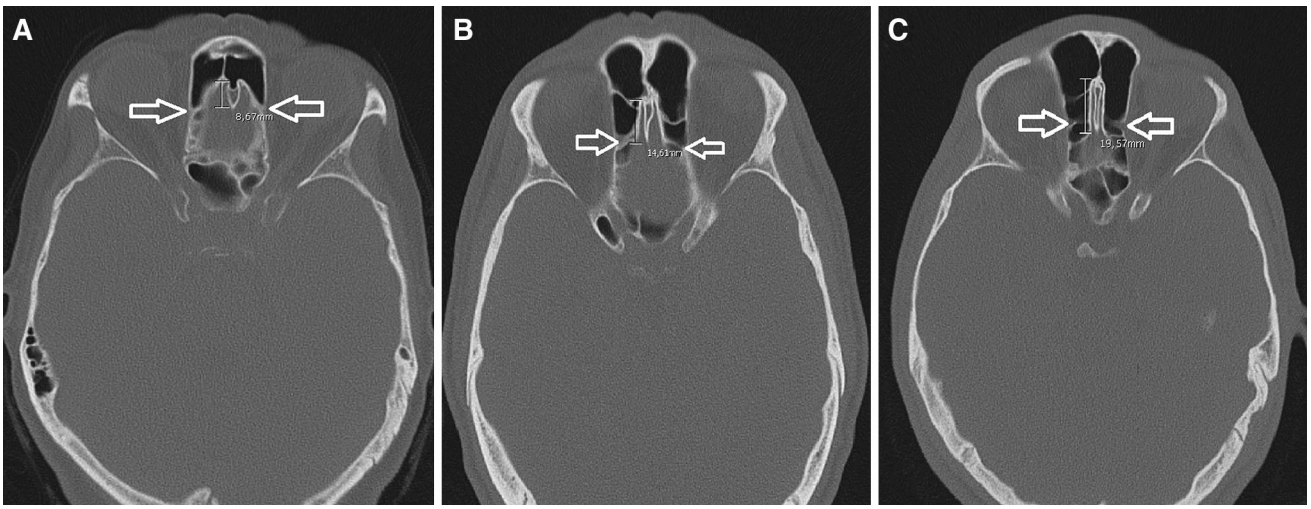

Fig. 1 **a** Cribriform plate with an anterior–posterior length of 6–10 mm (type 1) in axial section, **b** cribriform plate with an anterior–posterior length of 11–15 mm (type 2) in axial section, **c** cribriform plate with an anterior–posterior length of 16–20 mm (type 3) in axial section

Table 1 Relation between the cribriform plate's superior–inferior depth (Keros classification) and anterior–posterior length (Yenigun classification) and the arteria ethmoidalis anterior (AEA)'s visualization and direct penetration of the skull base

All patients	Right	Left	Total
Classification of cribriform plate's depth (Keros classification)			
Type 1 (0–3 mm)	25.5 % (47/184)	26.1 % (48/184)	26.0 % (95/368)
Type 2 (4–7 mm)	54.3 % (100/184)	56.5 % (104/184)	56.0 % (204/368)
Type 3 (8–16 mm)	20.1 % (37/184)	17.4 % (32/184)	18.9 % (69/368)
Relation between the cribriform plate's depth and AEA's visualization			
Type 1 (0–3 mm)	23.4 % (11/47)	25.0 % (12/48)	24.2 % (23/95)
Type 2 (4–7 mm)	56.0 % (56/100)	57.7 % (60/104)	56.8 % (116/204)
Type 3 (8–16 mm)	86.5 % (32/37)	78.1 % (25/32)	82.3 % (57/69)
Relation between the cribriform plate's depth and AEA's direct penetration of the skull base			
Type 1 (0–3 mm)	76.6 % (36/47)	75.0 % (36/48)	75.8 % (72/95)
Type 2 (4–7 mm)	44 % (44/100)	42,3 % (44/104)	43.1 % (88/204)
Type 3 (8–16 mm)	13.5 % (5/37)	21.9 % (7/32)	17.7 % (12/69)
Classification of cribriform plate's length (Yenigun classification)			
Type 1 (6–10 mm)	42.5 % (47/184)	41.1 % (48/184)	41.8 % (95/368)
Type 2 (11–15 mm)	52.0 % (100/184)	54.6 % (104/184)	53.3 % (204/368)
Type 3 (16–20 mm)	5.1 % (37/184)	4.7 % (32/184)	4.9 % (69/368)
Relation between the cribriform plate's length and AEA's visualization			
Type 1 (6–10 mm)	19.5 % (15/77)	19.5 % (15/77)	19.5 % (30/154)
Type 2 (11–15 mm)	76.5 % (75/98)	74.5 % (73/98)	75.5 % (148/196)
Type 3 (16–20 mm)	100 % (9/9)	100 % (9/9)	100 % (18/18)
Relation between the cribriform plate's length and AEA's direct penetration of the skull base			
Type 1 (6–10 mm)	80.5 (62/77)	80.5 (62/77)	80.5 (124/154)
Type 2 (11–15 mm)	23.5 % (23/98)	25.5 (25/98)	24.5 % (48/196)
Type 3 (16–20 mm)	0 % (0/9)	0 % (0/9)	0 % (0/9)

skull base rises steeply. This correlation has been found statistically significant (right: $p = 0.00$; left: $p = 0.00$) (Tables 1, 2).

Assessing the CT images of our 184 patients, supraorbital pneumatization was observed in 40.2 % of the cases (right: 39.7 %, left: 40.8 %). In the presence of supraorbital pneumatization, the AEA ran visibly inside the sinus in 75.0 % of cases (right: 72.7 %, left: 77.3 %), in the absence of supraorbital pneumatization, the figures were 25.0 % (right: 27.3 %, left: 22.7 %). This correlation has

Table 2 Association of the presence of Arteria ethmoidalis anterior (AEA) visualization with morphological variations in the adjacent structures

Variations	Visualization of AEA right (p)	Visualization of AEA left (p)
The association of superior–inferior depth of Cribriform plate	0.00**	0.00**
The association of anterior–posterior length of Cribriform plate	0.00**	0.00**
The association of pneumatization of supraorbital cell	0.00**	0.00**
The association of Agger nasi cell	0.84	0.36
The association of middle concha bullosa	0.79	0.72
The association of nasal septum deviation	0.45	0.39
The association of pneumatization of crista galli	0.91	0.82

Chi square test ** $p < 0.01$

been found statistically significant (right: $p = 0.00$; left: $p = 0.00$) (Table 2).

An agger nasi cell was found in 48.1 % of the cases, with similar rates on the right (47.8 %) and on the left (48.4 %). No statistically relevant correlation was found between presence of an agger nasi cell and AEA visualization (right: $p = 0.84$, left: $p = 0.36$) (Table 2).

For the pneumatization of the medial concha, a rate of 32.6 % was found, right (33.2 %) and left (32.1 %) being similar. No statistically relevant correlation was found between the presence of concha pneumatization and AEA visualization (right: $p = 0.79$, left: $p = 0.72$) (Table 2).

Septum deviation was found at a rate of 34.8 %. No statistically relevant correlation was found for either side between the presence of septum deviation and AEA visualization (right: $p = 0.45$, left: $p = 0.39$) (Table 2).

Crista galli pneumatization was found at a rate of 5.4 %. No statistically relevant correlation was found for either side between the presence of crista galli pneumatization and AEA visualization (right: $p = 0.91$, left: $p = 0.82$) (Table 2).

Discussion

The AEA is a major anatomical landmark running from the orbita to the anterior cranial fossa, lying in the ethmoidal sinus roof. Its injury by surgery or after trauma can cause serious epistaxis, retro-orbital hematoma, blindness, CSF leakage, meningitis, cerebral infection, and rarely intracranial bleeding [9]. Localization of the AEA in preoperative assessment is very important, given the differences in course and length. Three-dimensional spin digital subtraction angiography (DSA) is seen as the gold standard in the assessment of the AEA. However, this is an invasive method, involving the placement of a catheter in the femoral artery, the use of a contrast agent and an assessment through X-ray [10]. Micro-embolic events and the risk of potential cerebrovascular diseases are posing limits to the common use of this technique [11, 12].

The AEA extends from the ethmoidal roof in posterior-inferior direction toward the ethmoidal sulcus located in the lateral lamella of the cribriform plate [13]. Kainz and Stammberger reported that in cases of a low ethmoid roof, the anterior ethmoidal canal can enter directly into the skull base [14]. In our study, we also assessed the relation between AEA and the depth of the cribriform plate. According to Keros classification, with the increase of the cribriform plate's superior–inferior depth, the probability for the AEA to run visibly inside the ethmoidal sinus also increases. When the cribriform plate's superior–inferior depth decreases, the probability for the AEA to enter the skull base directly increases statistically significantly. As our study is the first to assess the course of the AEA with Keros classification, it contributes a novel approach to the literature.

Studies on the Keros classification usually research the frequency and differences of Keros types in societies and ethnic groups. Nitinavakarn et al. [15] found type 2 to be the most common one with 68.8 %, Basak et al. [16] among 64 child patients type 2 with 53 %, Jang et al. [17] in a patient group of 205 adults type 2 with 69.5 %, Anderhuber et al. [18] among 14-year-old child patients type 2 with 70.6 %, Souza et al. [19] in a study mainly involving adults type 2 with 73.3 %, Solares et al. [20] in a survey of 50 patients' CT images type 1 with 83 %, Adeel et al. [1] type 2 with 48.7 %. In our study, we found type 2 to be the most common one at a rate of 56 %.

When Keros [4] classified the superior–inferior depth of the cribriform plate in 1962, computed tomography was not used actively and three-dimensional images like those used today could not be obtained, while today we can assess anatomical structures and classifications in three dimensions, using contemporary technology. The lateral lamella of the cribriform plate is not only characterized by its depth but at the same time by its length in anterior–posterior

Table 3 Keros and Yenigun classification shows injury possibility of cribriform plate and arteria ethmoidalis anterior (AEA)

Keros classification	Score (mm)	Cribriform plate's depth	Injury possibility of Cribriform plate and AEA
Type-1	0–3	Low	Low
Type-2	4–7	Middle	Middle
Type-3	8–16	High	High
Yenigun classification	**Score (mm)**	**Cribriform plate's length**	**Injury possibility of Cribriform plate and AEA**
Type-1	6–10	Low	Low
Type-2	11–15	Middle	Middle
Type-3	16–20	High	High

direction. This is why three-dimensional approach is necessary today. In the axial paranasal CT, the anterior–posterior length of the cribriform plate was measured from the level where the course of the AEA had been traced. For this measurement, the endpoint of the crista galli was taken as the posterior border. The measurements in 184 patients resulted in a range between 6 and 20 mm. They were classified into three types, in analogy with the Keros classification, with a new "Yenigun classification" as type 1: 6–10 mm, type 2: 11–15 mm, and type 3: 16–20 mm. In our study, we assessed the relation between the AEA and the length of the cribriform plate. With increasing anterior–posterior length of the cribriform plate, the probability for the AEA to run visibly inside the sinus increases. When the anterior–posterior length of the cribriform plate decreases, the probability for the AEA directly to penetrate the skull base increases in a statistically significant way. We have also shown that the Yenigun classification defined in axial section carries clinical importance regarding the course of the AEA. We generated a clinical guideline showing injury possibility of cribriform plate and AEA in Keros and Yenigun classification (Table 3).

Moon et al. reported that the AEA runs freely inside the anterior ethmoid cells in only 11 % of the cases, while in 85.7 % it is found in direct contact with the skull base [21]. Souza et al. showed that the AEA runs freely inside the ethmoid sinus in 41 % of cases [5]. In this study, AEA was running freely inside the ethmoidal sinus in 53.8 % of the cases, and in 47.2 % it directly entered the skull base.

Several endoscopic studies have shown that in the presence of supraorbital ethmoidal sinus pneumatization (SOP), the position of the anterior ethmoidal artery from the skull base is more inferior than normal and it is running freely inside the ethmoidal sinus [5, 9, 22–25]. In our study, in the absence of supraorbital pneumatization, the AEA was running freely inside the ethmoidal sinus in 25 % of the cases. In case of supraorbital pneumatization, on the other hand, we found this situation approximately more than twice increased at 70 % (right: $p = 0.00$, left: $p = 0.00$).

Our study found no statistically significant relation between the presence of an agger nasi cell, medial concha pneumatization, septum deviation, and crista galli pneumatization on either side and the course of the AEA.

Conclusion

This study has demonstrated that with the increase of the superior–inferior depth and anterior–posterior length and the presence of supraorbital pneumatization, AEA is significantly more likely to be running freely inside the ethmoidal sinus, thus being more prone to being injured during surgery. With a new classification, we have shown that the length of the cribriform plate is as relevant clinically as is the depth, and three-dimensional assessment is therefore required. Careful dissection, surgical experience and awareness of anatomical surgical landmarks are very important in sinus surgery. In addition to these, we believe that knowledge of the course of the AEA and its correlation with surrounding anatomic structures will decrease the risk of complications in trauma, surgical, and endoscopic interventions and increase success rates.

Compliance with ethical standards

This article does not contain any studies with human participants or animals performed by any of the authors.

Funding source, financial disclosures None.

Research involving human participants and/or animals None.

Informed consent None (this is a retrospective study).

Conflict of interest All authors declare that they have no conflict of interest.

References

1. Adeel M, Ikram M, Rajput MS, Arain A, Khattak YJ (2013) Asymmetry of lateral lamella of the cribriform plate: a software-based analysis of coronal computed tomography and its clinical relevance in endoscopic sinus surgery. Surg Radiol Anat 35(9):843–847
2. McMains KC (2008) Safety in endoscopic sinus surgery. Curr Opin Otolaryngol Head Neck Surg 16(3):247–251
3. Stammberger HR, Kennedy DW, Anatomic Terminology Group (1995) Paranasal sinuses: anatomic terminology and nomenclature. Ann Otol Rhinol Laryngol Suppl 167:7–16
4. Keros P (1962) On the practical value of differences in the level of the lamina cribrosa of the ethmoid. Z Laryngol Rhinol Otol 41:809–813
5. Souza SA, Souza MM, Gregório LC, Ajzen S (2009) Anterior ethmoidal artery evaluation on coronal CT scans. Braz J Otorhinolaryngol 75(1):101–106
6. Araujo Filho BC, Weber R, Pinheiro Neto CD, Lessa MM, Voegels RL, Butugan O (2006) Endoscopic anatomy of the anterior ethmoidal artery: a cadaveric dissection study. Rev Bras Otorrinolaringol (Engl Ed) 72(3):303–308
7. Pandolfo I, Vinci S, Salamone I, Granata F, Mazziotti S (2007) Evaluation of the anterior ethmoidal artery by 3D dual volume rotational digital subtraction angiography and native multidetector CT with multiplanar reformations. Initial findings. Eur Radiol 17(6):1584–1590
8. Zinreich J (1998) Functional anatomy and computed tomography imaging of the paranasal sinuses. Am J Med Sci 316:2–11
9. Simmen D, Raghavan U, Briner HR, Manestar M, Schuknecht B, Groscurth P et al (2006) The surgeon's view of the anterior ethmoid artery. Clin Otolaryngol 31(3):187–191
10. Ding J, Sun G, Lu Y, Yu BB, Li M, Li L, Li GY, Peng ZH, Zhang XP (2012) Evaluation of anterior ethmoidal artery by 320-slice CT angiography with comparison to three-dimensional spin digital subtraction angiography: initial experiences. Korean J Radiol 13(6):667–673
11. Willinsky RA, Taylor SM, TerBrugge K, Farb RI, Tomlinson G, Montanera W (2003) Neurologic complications of cerebral angiography: prospective analysis of 2899 procedures and review of the literature. Radiology 227:522–528
12. Leffers AM, Wagner A (2000) Neurologic complications of cerebral angiography. A retrospective study of complication rate and patient risk factors. Acta Radiol 41:204–210
13. White DV, Sincoff EH, Abdulrauf SI (2005) Anterior ethmoidal artery: microsurgical anatomy and technical considerations. Neurosurgery 56(2 Suppl):406–410 **(discussion 406–410)**
14. Kainz J, Stammberger H (1988) The roof of the anterior ethmoid: a locus minoris resistentiae in the skull base. Laryngol Rhinol Otol (Stuttg) 67(4):142–149
15. Nitinavakarn B, Thanaviratananich S, Sangsilp N (2005) Anatomical variations of the lateral nasal wall and paranasal sinuses: a CT study for endoscopic sinus surgery (ESS) in Thai patients. J Med Assoc Thai 88(6):763–768
16. Başak S, Akdilli A, Karaman CZ, Kunt T (2000) Assessment of some important anatomical variations and dangerous areas of the paranasal sinuses by computed tomography in children. Int J Pediatr Otorhinolaryngol 55(2):81–89
17. Jang YJ, Park HM, Kim HG (1999) The radiographic incidence of bony defects in the lateral lamella of the cribriform plate. Clin Otolaryngol Allied Sci 24(5):440–442
18. Anderhuber W, Walch C, Fock C (2001) Configuration of ethmoid roof in children 0–14 years of age. Laryngorhinootologie 80(9):509–511
19. Souza SA, Souza MMA, Idagawa M, Wolosker AMB, Ajzen SA (2008) Computed tomography assessment of the ethmoid roof: a relevant region at risk in endoscopic sinus surgery. Radiol Bras 41(3):143–147
20. Solares CA, Lee WT, Batra PS, Citardi MJ (2008) Lateral lamella of the cribriform plate: software-enabled computed tomographic analysis and its clinical relevance in skull base surgery. Arch Otolaryngol Head Neck Surg 134(3):285–289
21. Moon HJ, Kim HU, Lee JG, Chung IH, Yoon JH (2001) Surgical anatomy of the anterior ethmoidal canal in ethmoid roof. Laryngoscope 111(5):900–904
22. Joshi AA, Shah KD, Bradoo RA (2010) Radiological correlation between the anterior ethmoidal artery and the supraorbital ethmoid cell. Indian J Otolaryngol Head Neck Surg 62(3):299–303
23. Jang DW, Lachanas VA, White LC, Kountakis SE (2014) Supraorbital ethmoid cell: a consistent landmark for endoscopic identification of the anterior ethmoidal artery. Otolaryngol Head Neck Surg 151(6):1073–1077
24. Floreani SR, Nair SB, Switajewski MC, Wormald PJ (2006) Endoscopic anterior ethmoidal artery ligation: a cadaver study. Laryngoscope 116:1263–1267
25. Lannoy-Penisson L, Schultz P, Riehm S, Atallah I, Veillon F, Debry C (2007) The anterior ethmoidal artery: radio-anatomical comparison and its application in endonasal surgery. Acta Otolaryngol 127:618–622